Lasing dynamics of super and sub luminal lasers

Jacob Scheuer[1,*] and Selim M. Shahriar[2,3]

[1]*School of Electrical Engineering, Tel-Aviv University, Ramat Aviv, Tel-Aviv 69978, Israel*
[2]*Dept. of Electrical Engineering and Computer Science, Northwestern University, Evanston, Illinois, 60208 USA*
[3]*Dept. of Physics and Astronomy, Northwestern University, Evanston, Illinois, 60208 USA*
[*]*kobys@eng.tau.ac.il*

Abstract: We study theoretically the lasing properties and the cavity lifetime of super and sub-luminal lasers. We find that obtaining the necessary conditions for superluminal lasing requires care and that a laser operating under these conditions can under some conditions tend towards bi-frequency lasing. In contrast, conditions for a subluminal laser are less stringent, and in most situations its steady-state properties are well predicted by the self-consistent single-frequency laser equations. We also study the relaxation time of power perturbation in super and sub-luminal lasers using a finite-difference-time-domain tool and present the impact of the lasing power, the group velocity and the dispersion properties of the cavity on the relaxation dynamic of such perturbations. For the subluminal laser, we find that the time constant changes by a factor that is close to the group index. In contrast, for the superluminal laser, we find that the time constant does not change by the factor given by the group index, and remains close to or above the value for an empty cavity. These finding may be interpreted to imply that the quantum noise limited linewidth of the subluminal laser decreases with increasing group index, while the same for the superluminal laser does not increase with decreasing group index. The implications of these findings on the sensitivity of sensors based on these lasers are discussed in details.

OCIS codes: (140.0140) Lasers and laser optics; (140.3560) Lasers, ring.

References and links

1. J. B. Khurgin and R. S. Tucker, *Slow Light: Science and Applications* (CRC Press, 2009).
2. J. Sharping, Y. Okawachi, and A. Gaeta, "Wide bandwidth slow light using a Raman fiber amplifier," Opt. Express **13**(16), 6092–6098 (2005).
3. D. Dahan and G. Eisenstein, "Tunable all optical delay via slow and fast light propagation in a Raman assisted fiber optical parametric amplifier: a route to all optical buffering," Opt. Express **13**(16), 6234–6249 (2005).
4. Y. Okawachi, M. S. Bigelow, J. E. Sharping, Z. Zhu, A. Schweinsberg, D. J. Gauthier, R. W. Boyd, and A. L. Gaeta, "Tunable all-optical delays via Brillouin slow light in an optical fiber," Phys. Rev. Lett. **94**(15), 153902 (2005).
5. K. Y. Song, M. Herráez, and L. Thévenaz, "Observation of pulse delaying and advancement in optical fibers using stimulated Brillouin scattering," Opt. Express **13**(1), 82–88 (2005).
6. Z. Zhu, D. J. Gauthier, and R. W. Boyd, "Stored light in an optical fiber via stimulated Brillouin scattering," Science **318**(5857), 1748–1750 (2007).
7. M. S. Bigelow, N. N. Lepeshkin, and R. W. Boyd, "Superluminal and Slow Light Propagation in a Room-Temperature Solid," Science **301**(5630), 200–202 (2003).
8. C. J. Chang-Hasnain, P.-C. Ku, J. Kim, and S.-L. Chuang, "Variable Optical Buffer Using Slow Light in Semiconductor Nanostructures," Proc. IEEE **91**, 1184 (2003).
9. J. Scheuer and M. S. Shahriar, "Trap-door optical buffering using a flat-top coupled microring filter: the superluminal cavity approach," Opt. Lett. **38**(18), 3534–3537 (2013).
10. H. Yum, X. Liu, Y. J. Jang, M. E. Kim, and S. M. Shahriar, "Pulse Delay Via Tunable White Light Cavities Using Fiber-Optic Resonators," J. Lightwave Technol. **29**(18), 2698–2705 (2011).
11. D. D. Smith, H. Chang, K. Myneni, and A. T. Rosenberger, "Fast-light enhancement of an optical cavity by polarization mode coupling," Phys. Rev. A **89**(5), 053804 (2014).
12. O. Kotlicki and J. Scheuer, "Wideband coherent perfect absorber based on white-light cavity," Opt. Lett. **39**(23), 6624–6627 (2014).

#251818 Received 12 Oct 2015; revised 8 Nov 2015; accepted 12 Nov 2015; published 8 Dec 2015

13. D. D. Smith, H. Chang, L. Arissian, and J. C. Diels, “Dispersion-enhanced laser gyroscope,” Phys. Rev. A **78**(5), 053824 (2008).
14. D. D. Smith, K. Myneni, J. A. Odutola, and J. C. Diels, “Enhanced sensitivity of a passive optical cavity by an intracavity dispersive medium,” Phys. Rev. A **80**(1), 011809 (2009).
15. J. Scheuer and M. Sumetsky, “Optical-fiber microcoil waveguides and resonators and their applications for interferometry and sensing,” Laser Photonics Rev. **5**(4), 465–478 (2011).
16. G. S. Pati, M. Salit, K. Salit, and M. S. Shahriar, “Demonstration of displacement–measurement–sensitivity proportional to inverse group index of intra-cavity medium in a ring resonator,” Opt. Commun. **281**(19), 4931–4935 (2008).
17. O. Kotlicki, J. Scheuer, and M. S. Shahriar, “Theoretical study on Brillouin fiber laser sensor based on white light cavity,” Opt. Express **20**(27), 28234–28248 (2012).
18. H. N. Yum, M. Salit, J. Yablon, K. Salit, Y. Wang, and M. S. Shahriar, “Superluminal ring laser for hypersensitive sensing,” Opt. Express **18**(17), 17658–17665 (2010).
19. S. Mookherjea, “Semiconductor coupled-resonator optical waveguide laser,” Appl. Phys. Lett. **84**(17), 3265–3267 (2004).
20. Y. Liu, Z. Wang, M. Han, S. Fan, and R. Dutton, “Mode-locking of monolithic laser diodes incorporating coupled-resonator optical waveguides,” Opt. Express **13**(12), 4539–4553 (2005).
21. Z. Zhou, J. Yablon, M. Zhou, Y. Wang, A. Heifetz, and M. S. Shahriar, “Modeling and analysis of an ultra-stable subluminal laser,” to appear in Optics Communications (http://arxiv.org/abs/1506.06379).
22. T. Lauprêtre, S. Schwartz, R. Ghosh, I. Carusotto, F. Goldfarb, and F. Bretenaker, “Anomalous ring-down effects and breakdown of the decay rate concept in optical cavities with negative group delay,” New J. Phys. **14**(4), 043012 (2012).
23. X. Han, H. Luo, T. Qu, Z. Wang, J. Yuan, and B. Zhang, “Theoretical design of a superluminal helium–neon ring laser via coupled passive cavities,” J. Opt. **16**(12), 125401 (2014).
24. T. Lauprêtre, C. Proux, R. Ghosh, S. Schwartz, F. Goldfarb, and F. Bretenaker, “Photon lifetime in a cavity containing a slow-light medium,” Opt. Lett. **36**(9), 1551–1553 (2011).
25. A. Wicht, K. Danzmann, M. Fleischhauer, M. Scully, G. Müller, and R.-H. Rinkleff, “White-light cavities, atomic phase coherence, and gravitational wave detectors,” Opt. Commun. **134**(1-6), 431–439 (1997).
26. D. D. Smith, H. Chang, K. Myneni, and A. T. Rosenberger, “Fast-light enhancement of an optical cavity by polarization mode coupling,” Phys. Rev. A **89**(5), 053804 (2014).
27. A. E. Siegman, *Lasers*, 2nd ed. (University Science Books, 1986).
28. R. M. Joseph, S. C. Hagness, and A. Taflove, “Direct time integration of Maxwell’s equations in linear dispersive media with absorption for scattering and propagation of femtosecond electromagnetic pulses,” Opt. Lett. **16**(18), 1412–1414 (1991).
29. A. Taflove and S. C. Hagness, *Computational Electrodynamics: The Finite-Difference Time-Domain Method*, 3rd ed. (Artech House Press, 2005).
30. M. O. Scully and W. E. Lamb, *Laser Physics* (Westview Press, 1974).
31. Y. Wang, Z. Zhou, J. Yablon, and M. S. Shahriar, “Effect of Multi-Order Harmonics in a Double-Raman Pumped Gain Medium For a Superluminal Laser,” Opt. Eng. **54**(5), 057106 (2015), doi:10.1117/1.OE.54.5.057106.
32. A. L. Schawlow and C. H. Townes, “Infrared and optical masers,” Phys. Rev. **112**(6), 1940–1949 (1958).
33. C. H. Townes, “Some applications of optical and infrared masers,” in *Advances in Quantum Electronics*, J.R. Singer, ed. (Columbia University Press, 1961), pp 1–11.
34. M. Lax, “Quantum noise X. Density-matrix treatment of field and population-difference fluctuations,” Phys. Rev. **157**(2), 213–231 (1967).
35. T. A. Dorschner, H. A. Haus, M. Holz, I. W. Smith, and H. Statz, “Laser gyro at quantum limit,” IEEE J. Quantum Electron. **16**(12), 1376–1379 (1980).
36. C. H. Henry, “Theory of the Linewidth of Semiconductor Lasers,” IEEE J. Quantum Electron. **18**(2), 259–264 (1982).
37. B. T. King, “Application of superresolution techniques to ring laser gyroscopes: exploring the quantum limit,” Appl. Opt. **39**(33), 6151–6157 (2000).
38. W. W. Chow, J. Gea-Banacloche, L. M. Pedrotti, V. E. Sanders, W. Schleich, and M. O. Scully, “The ring laser gyro,” Rev. Mod. Phys. **57**(1), 61–104 (1985).

1. Introduction

The ability to control the velocity of wave propagation has been the focus of numerous studies during the last two decades [1]. This interest stems both from the fundamental importance of the speed of light and from the diverse applications facilitated by the ability to control it. Indeed, studies in slow and fast light have initiated a variety of applications in diverse fields such as telecom, nonlinear optics, sensing and more [1-8]. In addition to the fundamental interest in sub/super luminal group velocity, cavities incorporating slow and fast light effects have tremendous potential for applications in many fields such as, sensing, data buffering, optical memories, true delay lines, etc. [9-24]. Fast light cavities are highly attractive for sensing [11,13-18] and buffering [9,10] applications, while slow-light cavities have interesting applications in sensing and low threshold and ultra-stable lasers [1,15,19,20,21].

While the properties of wave propagation in dispersive media and structures characterized by super or very sub luminal group velocity are well understood, the impact of such group velocities in both active and passive cavities is not obvious. In particular, the incorporation of slow/fast light media and structures in such cavities induces non-trivial impact on their fundamental properties such as cavity life-time, resonance frequencies, etc. The former becomes crucial in active cavities (i.e. lasers) in which the gain medium is also utilized for obtaining the desired dispersion properties. Consequently, parameters such as the roundtrip time and Q-factor, which are commonly considered as fixed properties of the "cold" cavity, become dynamic and dependent on the lasing conditions.

In this letter we present a theoretical study (analytic and numerical) of the lasing properties and dynamics of lasers incorporating intra-cavity fast/slow light medium. We calculate the dispersion relations (lasing frequency vs. cavity length) for both super and sub luminal lasers and obtain the range of parameters in which such lasing properties are obtained. We find that while subluminal lasers exhibit stable dynamical properties which are well predicted by the conventional laser equations, superluminal lasers (at least in the specific configuration studied here) are less stable and tend to exhibit bi-frequency lasing within the "superluminal" frequency range unless special means are employed (see Section 3). We also study the relaxation time of power perturbation in super and sub-luminal lasers, and investigate the impact of the lasing power, the group velocity and the dispersion properties of the cavity on the relaxation dynamic of such perturbations. Potential role of this relaxation time constant in determining the quantum noise limited linewidth of these lasers is also discussed.

The rest of this paper is arranged as follows. In Sec. 2 we present several configurations for obtaining super and subluminal group velocities in the laser cavity and discuss the analytic steady state solutions for the lasing properties in both cases. In Section 3 we present a finite-difference-time-domain (FDTD) analysis of the steady-state lasing as well as the dynamics of such lasers and in Section 4 we discuss the results and conclude.

2. Controlling the group index in the laser

In order to realize a sub/super luminal laser it is necessary to induce the required dispersive properties in the cavity. There are many different ways to realize such lasers and cavities [9,10,16-18,25,26,31], but here we consider a specific model where the gain profile consists of a combination of a wide gain peak with an additional narrow gain (absorption) line for obtaining the positive (negative) dispersion needed for obtaining sub (super) luminal group velocity. Thus, the complex dielectric coefficient of the medium in the cavity can be described as:

$$\varepsilon_r(\omega) = \varepsilon_\infty + \frac{\omega_0^2 \Delta\varepsilon_G}{\omega^2 + 2i\omega\Gamma_G - \omega_0^2} \pm \frac{\omega_0^2 \Delta\varepsilon_A}{\omega^2 + 2i\omega\Gamma_A - \omega_0^2}, \tag{1}$$

where $\Delta\varepsilon_{G,A}$ and $\Gamma_{G,A}$ correspond respectively to amplitude and linewidth of the broad gain (*G*) and the narrow gain/absorption (*A*) lines. The sign of the last term in the RHS of (1) determines whether that expression represents gain (plus sign) or absorption (minus sign). Figure 1 illustrates the gain and dispersion properties of such super and sub-luminal laser media. The set of parameters, indicated in the caption, correspond to those of Rb^{85} and Rb^{87} which is a very convenient set of materials for realizing super and sub-luminal laser systems [16, 18, 21, 31].

#251818 Received 12 Oct 2015; revised 8 Nov 2015; accepted 12 Nov 2015; published 8 Dec 2015

The steep dispersion curves depicted in Fig. 1 indicate strong dispersive properties - negative (superluminal group velocity) for the narrow absorption notch case and positive (subluminal group velocity) for the narrow gain peak. These dispersive properties have great impact on the lasing characteristics of sub/super luminal lasers as they can modify the free spectral range, the Q-factor, the relation between the cavity length, and the lasing frequency of the laser, etc.

Note that the extremely strong dispersion is obtained only at a relatively narrow bandwidth in the vicinity of the resonance of the narrow gain/absorption line. Another important point that must be noted is that the actual dispersion experienced by the light in sub/super luminal laser may differ substantially from the curves presented in Fig. 1 [18]. The reason for that is that gain saturation effects modify $\Gamma_{G,A}$ and $\Delta\varepsilon_{G,A}$ in (1) according to [27]:

$$\Delta\varepsilon_{G,A} = \frac{\Delta\varepsilon^0_{G,A}}{1 + I/I^{G,A}_{sat}};\ \Gamma_{G,A} = \Gamma^0_{G,A} \cdot \sqrt{1 + I/I^{G,A}_{sat}}, \tag{2}$$

where I_{sat} is the saturation power which can be different for each gain/absorption line. Thus, in order to obtain the dispersive properties of such lasers it is necessary to solve the self-consistent laser equations to obtain the relation between the cavity length and the lasing frequency and, hence, the saturated gain dispersion relations.

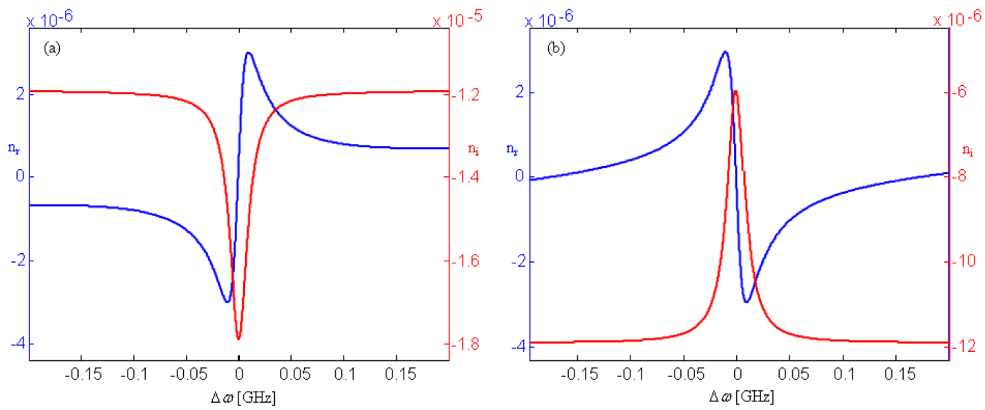

Fig. 1. Real (blue) and imaginary (red) parts of the refractive index for subluminal (a) and superluminal (b) laser media. $\varepsilon_\infty = 1$, $\Gamma_G = 6$GHz, $\Gamma_A = 0.01$GHz, $\Delta\varepsilon_G = 1.52\text{x}10^{-7}$, $\Delta\varepsilon_A = 1.27\text{x}10^{-10}$.

2.1 Superluminal laser

To obtain a superluminal laser ($v_g > c$) it is necessary to have negative sign for the last term in the RHS of (1), i.e. a narrow absorption line is needed. Such absorption line can be introduced into the cavity by means of e.g. an atomic vapor cell [18] or an under-coupled intra-cavity resonator [17]. There is, however, a subtle difference between these implementations. In the first one, the absorption line is of a *saturating* type and its linewidth and absorption are affected by the laser intensity. In the second, however, the absorber is completely passive and is, therefore, independent of the lasing power. Despite this difference, the properties of the two implementations are very similar and throughout this paper we focus mostly on the second (non-saturating absorber) approach as it is simpler to analyze.

Under lasing conditions, the dispersive properties of the refractive index of the laser medium are determined primarily by the first and last terms in (1). The impact of the broad gain is relatively negligible because it is saturated and its derivative with respect to the frequency is small. Assuming the last two terms in (1) are small compared to ε_∞ (see Fig. 1),

#251818 Received 12 Oct 2015; revised 8 Nov 2015; accepted 12 Nov 2015; published 8 Dec 2015

the real part of the refractive index in the vicinity of the resonance ω_0 can be approximated as:

$$n_r(\omega) \approx \varepsilon_\infty - \frac{1}{4}\cdot\frac{\omega_0 \Delta\varepsilon_A \cdot \Delta\omega}{\Delta\omega^2 + \Gamma_A^2}, \tag{3}$$

where $\Delta\omega = \omega - \omega_0$. The group index at the resonance of the absorption line is, therefore, given by:

$$n_g(\omega_0) = \varepsilon_\infty + \omega_0 \left.\frac{dn_r}{d\omega}\right|_{\omega_0} = \varepsilon_\infty - \frac{\omega_0^2 \Delta\varepsilon_A}{4\Gamma_A^2}. \tag{4}$$

Equation (4) provides a simple design rule for obtaining any desired group index. In particular, for $n_g = 0$ (i.e. $v_g \to \infty$) it is necessary for the absorption line to satisfy $\Delta\varepsilon_A = 4\Gamma_A^2 \varepsilon_\infty / \omega_0^2$. Note that, in principle, any desired group index can be obtained (positive, zero or negative) where the only restriction is that the overall roundtrip gain in the cavity must exceed the cavity loss at the center of the net gain profile.

The lasing frequency and the intensity can be obtained by solving the self-consistent, single frequency laser equation:

$$\exp\left(ik_0 nL - \alpha L/2\right) = 1, \tag{5}$$

where L is the roundtrip length, k_0 is the vacuum wavenumber, α is the roundtrip loss (comprising both mirror losses and material absorption) and $n = n_r + i \cdot n_i$ is the *complex* refractive index which can be derived from (1) and (2):

$$\begin{aligned} n_r(\Delta\omega) &= 1 + \frac{\omega_0 \Delta\varepsilon_G \cdot \Delta\omega}{4(\Delta\omega^2 + \Gamma_G^2)} - \frac{\omega_0 \Delta\varepsilon_A \cdot \Delta\omega}{4(\Delta\omega^2 + \Gamma_A^2)} \\ n_i(\Delta\omega) &= -\frac{\omega_0 \Delta\varepsilon_G \Gamma_G}{4(\Delta\omega^2 + \Gamma_G^2)} + \frac{\omega_0 \Delta\varepsilon_A \Gamma_A}{4(\Delta\omega^2 + \Gamma_A^2)}. \end{aligned} \tag{6}$$

Note that in (6) we have assumed $\varepsilon_\infty = 1$. In addition, it should be stressed that the gain ($\Delta\varepsilon$) and linewidth (Γ) parameters in (6) are modified by the lasing intensity according to (2). Figure 2 depicts the effective dispersion relation (expressed as the lasing frequency shift vs. cavity length shift) for a superluminal laser with the following parameters: Γ_G = 6THz, Γ_A = 10GHz, $\Delta\varepsilon_G$ = 1.52x10^{-7}, $\Delta\varepsilon_A$ = −7.88x10^{-11}, $I_{sat}^G = 5$, and as mentioned above, the absorption line is of non-saturating type. We choose the rather broad linewidths (in comparison to those used in Fig. 1) in order to compare the analytic results with the numeric results discussed in section 3. The broader linewidth allow for faster dynamics and relaxation which is essential for reasonable computational times. The group index is extracted from the dispersion relations [18]: $n_g = \Delta\nu / \Delta L \cdot L_0 / \nu_0$. The base cavity length L_0 is set such that the cavity resonance coincides with the peak of the gain and the maximal absorption of the additional absorption line, ν_0, given by L_0 = 25μm and $\nu_0 = 300\text{THz}$. The choice of such a small length for the laser cavity was dictated by the need to accommodate the modeling of the dynamic relaxation process in a realistic manner, as discussed further later. In the vicinity of the absorption resonance the slope of the dispersion relation increases, corresponding to a group index of n_g~0.3 for the chosen set of parameters.

#251818 Received 12 Oct 2015; revised 8 Nov 2015; accepted 12 Nov 2015; published 8 Dec 2015

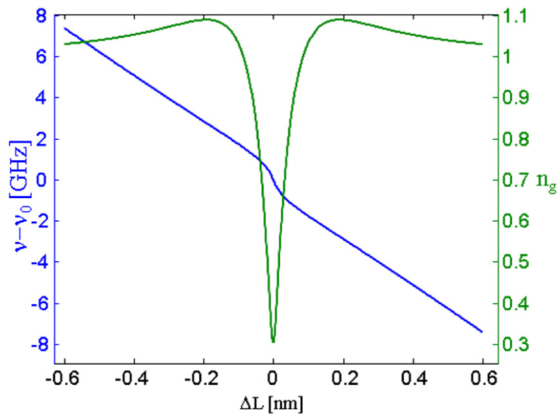

Fig. 2. Lasing frequency detuning (blue) and corresponding group index (green) of a superluminal laser. See text for the specific parameters.

2.2 Subluminal group velocity

To obtain a subluminal laser ($v_g<c$), the sign of the last term in the RHS of (1) has to be positive. Intuitively, this corresponds to an additional narrow gain line although it is possible to obtain a subluminal laser by introducing an intra-cavity over-coupled cavity (which essentially introduces additional loss).

The analysis of a subluminal laser [21] is essentially similar to that of a superluminal laser described above except that the sign of $\Delta\varepsilon_A$ in Eqs. (3-6) is negative and the corresponding group index is larger than 1. In addition, for the implementation employing an additional narrow gain line, it is necessary to introduce saturation into that line. Figure 3(a) depicts the dispersion relation for a subluminal laser with the following parameters: Γ_G = 6THz, Γ_A = 1.4GHz, $\Delta\varepsilon_G$ = 1.22x10^{-7}, $\Delta\varepsilon_A$ = 1.42x10^{-11}, $I_{sat}^G = 5$, and $I_{sat}^A = 500$ (the rest of the parameters are identical to those of Fig. 2). The choice of a relatively large saturation power for the narrow gain line is dictated by the need to ensure that this line is not broadened too much due to saturation effects.

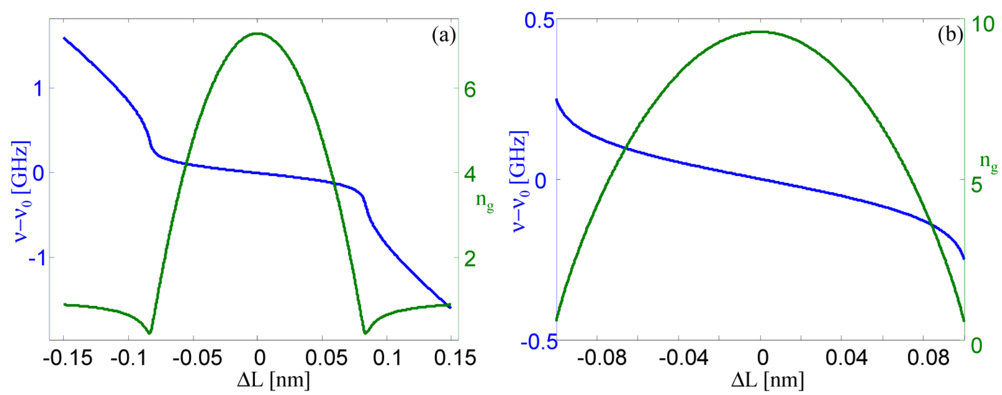

Fig. 3. Lasing frequency detuning (blue) and corresponding group index (green) of a subluminal laser comprising (a) an additional narrow gain line and (b) an intra-cavity passive over-coupled resonator (b).

Here, in the vicinity of the peak of the narrow gain line, the slope of the dispersion relation is very shallow, corresponding to a group index of n_g~7.3 for the chosen set of parameters. For the purpose of comparison, we present in Fig. 3(b) a similar plot for a

#251818 Received 12 Oct 2015; revised 8 Nov 2015; accepted 12 Nov 2015; published 8 Dec 2015

subluminal laser comprising a passive over-coupled intra-cavity resonator as a phase component. The system parameters are similar to those of Fig. 3(a) except that $\Delta\varepsilon_A = 1.89\text{x}10^{-11}$. Because the phase component is passive, its linewidth is not broadened due to the power in the cavity, thus yielding a larger group index of n_g~9.6.

3. FDTD simulations

3.1 Numerical model

To verify the results of Section 2 and to investigate the dynamics of sub/super luminal lasers we have expanded the numerical model presented in [28] to include multiple gain and absorption lines, including saturation effects. The implementation is straightforward but rather laborious as a 4th order difference equation is needed to model the complex constitutive relations between the electric and the displacement fields. The saturation effects are introduced by evaluating the intensity in the cavity at each time step and modifying the small signal gain/absorption and linewidth according to (2).

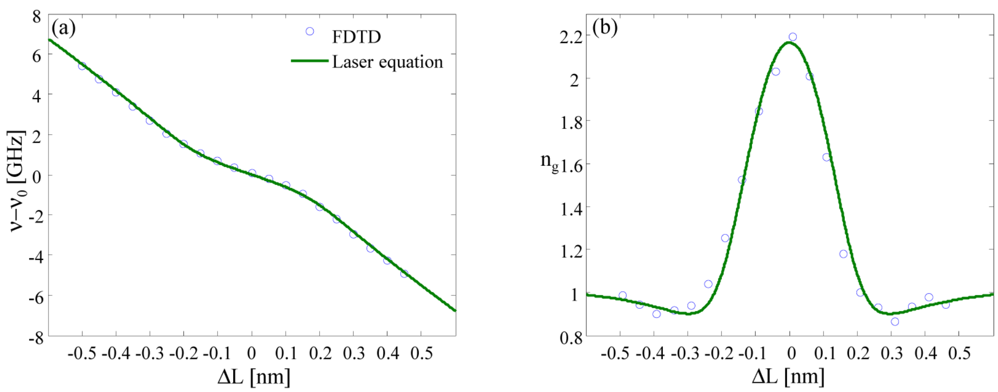

Fig. 4. Comparison between the dispersion relations (a) and the group index (b) obtained by FDTD simulations (circles) and the self-consistent laser equation solutions (solid line).

To avoid spatial hole burning effects due to counter-propagating waves, a 1D ring cavity is modeled by employing cyclic boundary conditions at the ends of the calculation window. An additional over-all roundtrip loss of 0.25% is introduced to account for output coupling from the laser. The simulation is seeded by a short, broadband and low-power pulse and run until a steady-state is reached. It should be noted that the implementation of the gain (and absorption) lines as complex dielectric coefficients implicitly assumes that the gain dynamics is much faster than the cavity roundtrip time. While this assumption has no impact on the steady-state solution of the laser system, it might affect the transient phenomena and the dynamics of the electromagnetic field in the laser. Thus, the parameters of the cavity are chosen such that its Q-factor is large and the implicit assumption on the gain dynamics is satisfied. In order to carry out a computation that is not constrained by this assumption on the gain dynamics, it is necessary to consider an explicit atomic model for the system (see e.g., [18,21,31]), and solve the density matrix equations at each point in space and time. Such an analysis is extremely time consuming, and would be carried out in the near future.

3.2 Steady-state lasing and dispersion relations

This section is separated into two scenarios: subluminal and superluminal lasers. As mentioned in Section 2 above, obtaining highly subluminal lasing requires the introduction of a narrow line gain on top of a broad gain or an over-coupled resonator into the laser cavity. Note that obtaining a large group index using a single, narrow, gain line is difficult due to the broadening induced by gain saturation effects. This is because the inherent broadening effect

#251818 Received 12 Oct 2015; revised 8 Nov 2015; accepted 12 Nov 2015; published 8 Dec 2015

which is accompanied by saturation as seen in Eq. (2). To avoid that, it is necessary to use two gain lines where saturation affects primarily the broad line while the narrower line remains *unsaturated* and able to produce the large group index. Clearly, this issue does not apply to the intra-cavity resonator implementation. Figure 4 depicts a comparison between the dispersion relations and the corresponding group index calculated by the laser equations to those calculated by FDTD simulations. The laser parameters are Γ_G = 6THz, Γ_A = 10GHz, $\Delta\varepsilon_G$ = 1.52x10^{-7}, $\Delta\varepsilon_A$ = 1.27x10^{-10}, $I_{sat}^{G}=5$, and $I_{sat}^{A}=500$. Here, υ_0 corresponds to the lasing frequency when the cavity length is set to the nominal length of L_0 = 25μm (i.e. ΔL = 0), and the peak of the narrow gain line coincides with the empty cavity resonance. The good agreement between the simulations and the solutions of the self-consistent laser equations is evident, where the slight differences are attributed to the numerical dispersion of the FDTD algorithm [29]. At the center of the narrow gain peak, a group index of n_g = 2.2 is obtained. We note that the choice to present a relatively modest group index here stems from the practical reason of keeping the computational time to be manageably small. A very large group index implies that the shift in the lasing frequency due to a change in the cavity length is very small, thus necessitating extremely long FDTD runs in order to determine that frequency with sufficient accuracy. Nevertheless, the obtained change in the group index due to the gain dispersion is larger than the group index of the empty cavity, and the excellent agreement between the simulations and the laser equation based analysis indicate that the concept is valid also for substantially larger group indices [18].

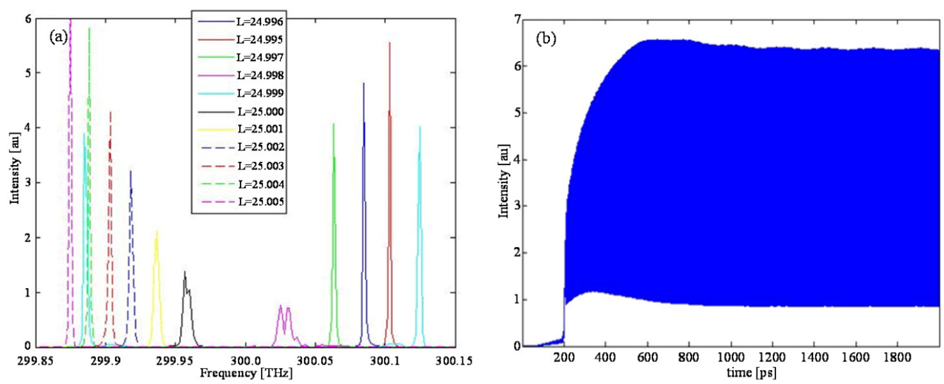

Fig. 5. (a) Steady-state spectra of a superluminal laser for various cavity length detuning; (b) temporal evolution of the intensity at the center of the cavity for ΔL = 0.

While the properties of subluminal lasers are described well by the self-consistent laser equation, the superluminal laser exhibits richer and more complex dynamical properties. Obtaining a superluminal laser calls for introducing a narrow absorption line within the cavity. In contrast to the subluminal laser case, where the large group index is associated with additional gain (at least for one of the implementations), the introduction of an intra-cavity absorption line requires special care in order to ensure that the over-all gain at the center of the absorption line exceeds the losses.

Figure 5(a) depicts the steady-state spectra of a superluminal laser as a function of the cavity length detuning. The parameters for the laser are: Γ_G = 6THz, Γ_A = 10GHz, $\Delta\varepsilon_G$ = 1.91x10^{-5}, $\Delta\varepsilon_A$ = −9x10^{-11}, and $I_{sat}^{G}=5$ (the absorption line is non-saturating). As can be expected, when the lasing frequency approaches the absorption notch, υ_0, the lasing intensity decreases due to the larger losses. However, when the cavity resonance coincides with the absorption notch, where the group index is expected to be below 1, the laser appears to lase at two frequencies simultaneously (cyan line in Fig. 5(a)). This is despite the fact that the gain is sufficient to maintain lasing at υ_0 and that none of the lasing frequencies are resonances of

#251818 Received 12 Oct 2015; revised 8 Nov 2015; accepted 12 Nov 2015; published 8 Dec 2015

the cavity (including the gain/loss dispersion). This is a rather unexpected result because the self-consistent laser equation does support a single wavelength lasing solution at υ_0 when the cavity detuning is zero. Figure 5(b) depicts the temporal evolution of the intensity at the center of the laser cavity for zero cavity detuning. Shortly after switch-on the power in the cavity starts oscillating, indicating the existence of two optical frequencies in the cavity. The evolution of the power shown in Fig. 5(b) suggests that the lasing solution at υ_0 is unstable, at least in the case where it evolves from zero power initial conditions.

To investigate further the possibilities to obtain single wavelength lasing at n_g<1 we have considered the situation where the absorption notch is introduced adiabatically. First, stable single-frequency lasing is established in a conventional laser (i.e. without the additional absorption line - $\Delta\varepsilon_A = 0$) and then the absorption is slowly increased, letting the lasing solution stabilize before further increasing the absorption. Following this procedure, we were able to obtain single frequency lasing at υ_0 with the following parameters: Γ_G = 6THz, Γ_A = 10GHz, $\Delta\varepsilon_G = 1.27\text{x}10^{-5}$, $\Delta\varepsilon_A = -1.13\text{x}10^{-8}$, and $I_{sat}^G = 5$. From this starting point, we were able to obtain the dispersion relation of the superluminal laser by changing the cavity length and detuning its resonance frequency. For example, in the case where the absorption is introduced via the Raman depletion process [18], this approach can be readily implemented by controlling the power of the Raman probe and the optical pump used to generate the Raman depletion.

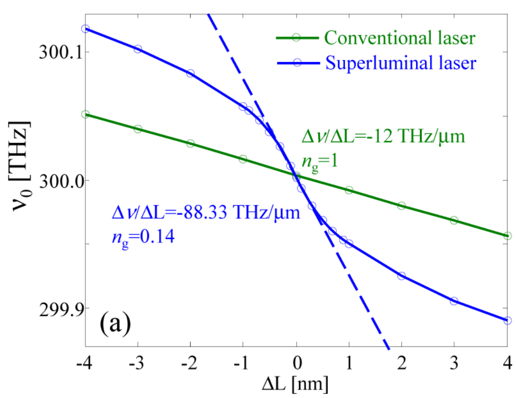

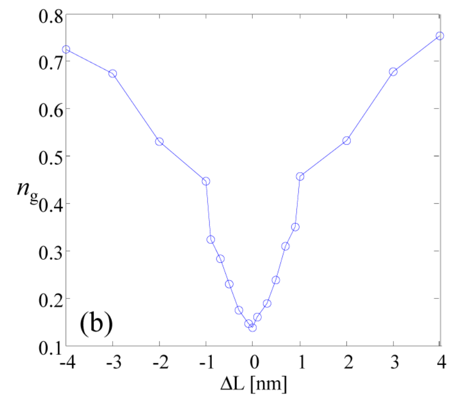

Fig. 6. (a) Comparison between the dispersion relation of a superluminal laser (blue) and that of a conventional one (green); (b) Corresponding group index vs. cavity length detuning

Figure 6(a) compares the dispersion relations obtained for the superluminal laser using the approach described above to that of a conventional laser of identical dimensions and pump parameters. The slope of the superluminal laser curve at zero detuning is approximately 7 times steeper than that of the conventional laser, indicating a group index of $n_g = 0.14$. Figure 6(b) depicts the group index corresponding to the dispersion relations of the superluminal laser. As can be expected, the small group index is obtained only in the vicinity of the zero detuning point (compare e.g. to Fig. 2).

The superluminal laser described above exhibits lasing solution with group indices below 1, which seems to be stable to sufficiently small perturbations (see also Section 3.3 below). Nevertheless, an exhaustive numerical study of the electric field dynamics in such superluminal lasers reveals that lasing with n_g~0 is in general an unstable solution which tends to break into bi-frequency lasing. We note that the dispersion relations depicted in Fig. 6 were obtained close to the threshold pump level and that attempts to obtain similar dispersion curves for substantially larger pump values and smaller group indices resulted in a bi-frequency lasing as shown in Fig. 5. To illustrate this, we present in Fig. 7 the evolution of

#251818 Received 12 Oct 2015; revised 8 Nov 2015; accepted 12 Nov 2015; published 8 Dec 2015

the power in the laser corresponding to Fig. 6 (ΔL = 0) when the pump level is slightly increased ($\Delta\varepsilon_G = 1.91\text{x}10^{-5}$). Following the increase in the pump level the power in the cavity begins to oscillate with increasing amplitude (clear sign of modulation instability), stabilizing to a power level which is approximately 4 times larger than that of the initial level. The spectrum of the steady state (see inset) consists of two frequencies which are equally detuned from resonance (by ~138GHz).

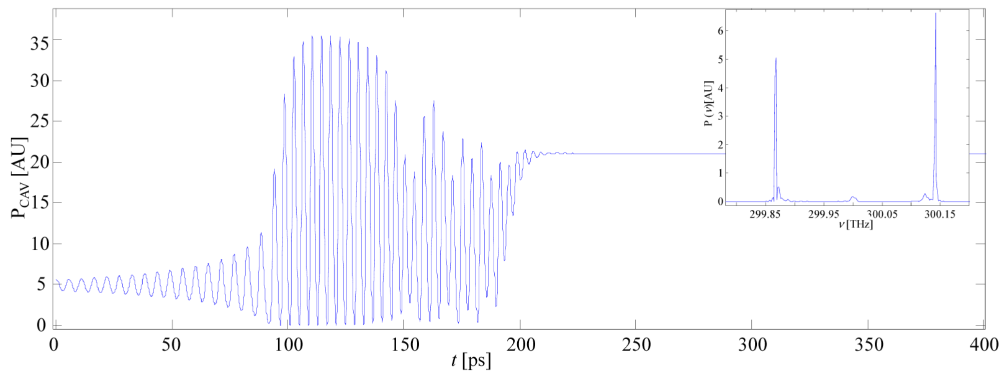

Fig. 7. Temporal evolution of the power in the cavity of a superluminal laser when the pump level is increased. Inset: steady state spectrum (for t>220ps).

Similar dynamics is observed when attempting to decrease the group index by increasing the depth of the absorption notch. Thus we can conclude that stable superluminal lasing solutions are possible if the group index is non-vanishing and close to the threshold pump levels. We would like to recall here that this computation is carried out under the assumption that the gain dynamics is much faster than the cavity round trip time. It is not obvious whether the tendency for the superluminal laser to break into bi-frequency lasing would hold when this assumption is not satisfied. As indicated earlier, a more comprehensive calculation that does not make this assumption, and solves the density matrix at each space and time point, will be carried out in the near future to address this issue. In addition, we would like to point out that the use of a superluminal laser for precise detection of displacement or rotation is possible even if it operates as a bi-frequency laser, since the spectrum of the laser is deterministic. Specifically, it would involve the measurement of multiple beat frequencies between two counter-propagating superluminal lasers, rather than a single one.

To complement the study, we consider the case of a superluminal laser comprising a saturated absorption line which can be produced, for example, via the process of Raman depletion in Rb vapor [18]. Similar to the case of the superluminal laser configuration discussed above, some care is needed in order to ensure that such a system would operate in the superluminal range. As in the subluminal case, this requires the saturation power of the absorption notch to be much larger than that of the gain. Therefore, we choose $I_{sat}^{A} = 500$ and the rest of the parameters are identical to the case presented in Fig. 6.

Figure 8(a) depicts the dispersion relations obtained for the superluminal laser with a saturating absorption line as calculated by FDTD. Figure 8(b) depicts the group index corresponding to the dispersion relations, indicating a group index of n_g = 0.23 when the cavity length is tuned to resonate at the center of the absorption line. Note that the minimal group index for this configuration is larger than that of the corresponding scheme comprising a non-saturating notch, although the parameters of the schemes are identical. The reason for the difference stems from the saturation of the absorption which leads to higher lasing power (under the same pump conditions) and broadening of the notch. As a result, the roundtrip phase in the cavity is undercompensated and the corresponding group index is larger.

#251818 Received 12 Oct 2015; revised 8 Nov 2015; accepted 12 Nov 2015; published 8 Dec 2015

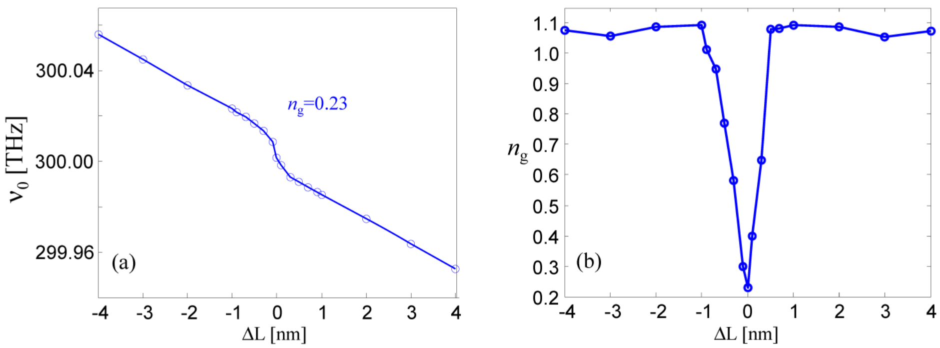

Fig. 8. (a) Dispersion relation of a superluminal laser with a saturating absorption line; (b) Corresponding group index vs. cavity length detuning

Except for the slight difference in the minimal group index, the dynamical properties of the saturating notch superluminal laser configuration are similar to those of the non-saturating absorption one. The plots depicted in Fig. 8 were obtained in a similar manner to those shown in Fig. 6, where an attempt to turn on the laser in "superluminal" configuration resulted in bi-frequency lasing.

3.3 Dynamic response to perturbations

We complete the analysis of superluminal and subluminal lasers by investigating the relaxation dynamics of these lasers following small perturbations. There are several reasons for performing such a study. First, it provides a quantitative measure of the stability properties of the lasing solutions. This is particularly important for the superluminal laser case which is found to be stable only within a narrow range of parameters. Second, such analysis can shed some light on the ability to describe such highly dispersive lasers by the semi-classical equations of motion that are commonly used for effectively single mode ring lasers [30]. These equations describe the temporal evolution of the field amplitude and phase in the cavity as a function of the gain properties, the resonance frequency and the empty cavity Q-factor. The evaluation of the last parameter (the Q) becomes problematic in highly dispersive lasers because it depends on the roundtrip losses and the cavity roundtrip time, which in turn is influenced by the group velocity in the laser. Because of dispersion, the group velocity in the laser can differ substantially from that in the empty cavity. Thus, the impact of the gain cannot be neglected when considering the roundtrip time. This issue is particularly important for superluminal lasers in which the group velocity can, under some conditions, far exceed the vacuum speed of light. If one were to assume, naively, that the cavity round trip time corresponds to the cavity length divided by this group velocity, one would be led to the clearly unphysical conclusion that the energy in the cavity flows at a velocity exceeding the vacuum speed of light. In order to circumvent such conclusions, it is thus necessary to identify an alternative approach for obtaining the time constant pertaining to the fluctuations in the laser by investigating the relaxation dynamics of small perturbations explicitly, via numerical analysis.

Another important aspect of the cavity lifetime (or, equivalently, the Q-factor), which directly depends on the group velocity in the cavity, is its impact on the quantum noise limited linewidth, also known as the Schawlow-Townes linewidth (STL) [32]:

$$\gamma_{ST} = \frac{h\omega_0}{2\tau_c^2 P_{out}}, \tag{7}$$

where ω_0, τ_c and P_{out} are, respectively, the lasing frequency, the lifetime of a spontaneously emitted photon in the cavity, and the power emitted from the cavity. In order to determine this linewidth it is necessary to determine the value of τ_c – a task that, as explained above, is fraught with potential complications for sub/super luminal lasers. Before proceeding further, we note that, for metrological applications, such as in rotation sensing, a more relevant parameter is the uncertainty in the measured value of the center frequency of the laser. This uncertainty, which we call $\Delta\omega_{CF}$ is given, in the quantum noise limit, by the geometric mean of the STL and the measurement bandwidth, which is the inverse of the measurement time, τ [31,31-38]:

$$\Delta\omega_{CF} = \sqrt{\gamma_{ST}/\tau} = \frac{1}{\tau_C}\sqrt{\frac{\hbar\omega_o}{2P_{out}\tau}}. \tag{8}$$

Thus, the measurement sensitivity/accuracy is inversely proportional to τ_c .

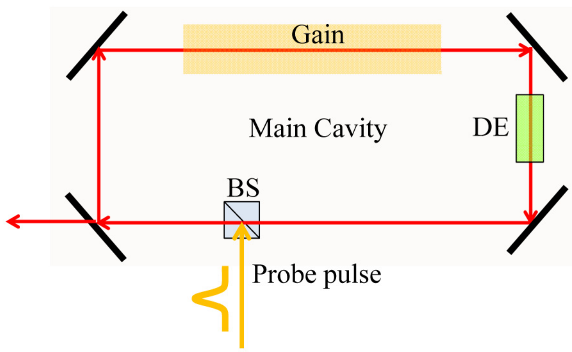

Fig. 9. Schematic of the relaxation dynamic calculation concept. DE – Dispersive Element; BS – Beam Splitter.

We study the relaxation of sub/super luminal lasers following a small perturbation consisting of a short, low-power, pulse of light which is injected into the cavity during lasing action. A schematic of the concept is illustrated in Fig. 9: First, the simulation is run until steady-state is reached. Then a short a low-power pulse is injected into the cavity while the power in the laser is monitored until the transients relax and steady-state is reached again. The dispersive element in Fig. 8 can provide negative, positive or no dispersion in order, respectively, to model a superluminal, subluminal or conventional laser.

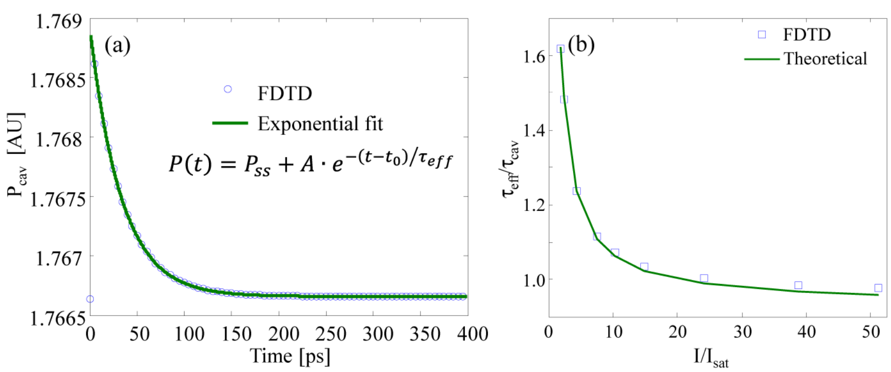

Fig. 10. (a) Relaxation dynamics of the power in a conventional laser following perturbation: FDTD simulation (circles) and exponential decay fit (solid line); (b) dependence of the effective relaxation time on the power in the laser: FDTD simulation (squares) and theoretical curve based on Eq. (11).

In order to verify the relations between the relaxation time obtained from the simulations and the corresponding cavity lifetime, we first study a conventional laser where no dispersive element is introduced into the cavity and $n_g = 1$. Figure 10(a) depicts an FDTD simulation of the relaxation of the power in a conventional laser to the steady-state solution and an exponential fit. The excellent agreement indicates that the relaxation is of exponential nature and allows of extracting the relaxation time τ_{eff}.

Figure 10(b) depicts the dependence of the extracted relaxation time on the power in the cavity (normalized to the saturation power). The plot shows that the relaxation time is larger for low power level and that it decreases and reaches a constant value, which is similar to the empty cavity lifetime, when the power in the cavity is increased (i.e. larger pumping). To understand the relations between the cavity power and the relaxation time and to establish the relations between that time and the empty cavity lifetime we consider the equation of motion for the intensity in the cavity:

$$\dot{I} = -\frac{1}{\tau_{cav}}\left[1-\frac{Q\chi_0''}{1+I}\right]\cdot I, \tag{9}$$

where $I = |E|^2/|E_{sat}|^2$ is the lasing intensity normalized to the saturation intensity, Q is the quality factor, $\chi'' = \chi_o''/(1+I)$ is the imaginary part of the electric susceptibility, and τ_{cav} is the empty cavity lifetime. At steady state, Eq. (9) yields the normalized lasing intensity I_0. Now, consider a small perturbation of the power in the cavity: $I = I_0 + \Delta I$. Substituting the expression for I into Eq. (9) yields an evolution equation for the perturbation:

$$\frac{d}{dt}\Delta I = -\frac{1}{\tau_{cav}}\cdot\frac{I_0}{1+I_0}\Delta I. \tag{10}$$

Equation (10) indicates that the power perturbation relaxes exponentially to the steady-state level where the relaxation time constant is given by:

$$\tau_{eff} = \frac{1+I_0}{I_0}\tau_{cav}. \tag{11}$$

The relaxation time τ_{eff} is related directly to the empty cavity lifetime τ_{cav} but also depends on I_0. For the case where $I_0 \ll 1$, corresponding to the threshold lasing condition, τ_{eff} is inversely proportional to I_0. However, as the intensity in the cavity is increased far beyond the saturation intensity (i.e., $I_0 \gg 1$), τ_{eff} converges to τ_{cav}. Figure 10(b) compares the relaxation time calculated by FDTD to Eq. (11), demonstrating excellent agreement (no parameters fit). We therefore conclude that the relaxation time obtained by the FDTD simulation yields the effective cavity lifetime.

Before proceeding further, we consider first the physical meaning of this increase in the effective decay time near threshold. The highly saturated limit ($I_0 \gg 1$) corresponds to a situation where the value of the gain per pass, which is given by $\xi\chi''$ (where ξ is a proportionality constant that depends on the cavity length) is reduced from $\xi\chi_0''$ by the factor of $(1 + I_0)\approx I_0$. This is balanced by the loss per pass, which is given by ξ/Q. However, for the near-threshold case ($I_0 \ll 1$), the gain per pass, which is given by $\xi\chi_0''$, still has to match ξ/Q. Therefore, in this case, the value of $\xi\chi_0''$, and therefore of χ_0'', is much smaller. Thus, we have two distinctly different situations. In the highly saturated case, the gain per pass depends hyperbolically on I_0, while for the near-threshold case, the gain per pass is essentially independent of I_0. As a result, the differential gain (i.e., the small signal gain) per pass differs for these two cases, while the differential loss per pass is the same. Specifically, for the highly saturated case, the differential gain is much smaller than the differential loss; as a result, following a perturbation, the laser reaches equilibrium at the rate of the differential loss, which is the same as that for an empty cavity. For the near-threshold case, the differential gain is higher, and the difference between the differential gain and the differential loss is much smaller; as a result, following a perturbation, the laser reaches equilibrium more slowly, at a rate that is smaller by the factor of I_0.

It should be noted that the expression in Eq. (11) for the effective decay time implies a curious conclusion regarding γ_{ST} and $\Delta\omega_{CF}$ for a non-dispersive laser if we use this effective time constant as the cavity decay time for a spontaneously emitted photon (i.e., substitute τ_{eff} for τ_c), in Eqs. (7) and (8). Specifically, near threshold (i.e., for I_o<<1), the value of γ_{ST} is expected to be smaller than the conventional value by a factor of I_0^2, and the value of $\Delta\omega_{CF}$ is expected to be smaller than the conventional value by a factor of I_o. Physically, these reductions in γ_{ST} and $\Delta\omega_{CF}$ may be interpreted as follows. The ratio of the rate of spontaneous emission into the lasing mode and the stimulated emission is given by 1/<n>, where <n> is the mean photon number in the laser. Since τ_{eff} is the effective decay rate for each photon in the laser, and the intensity in steady state is a constant, the rate of stimulated emission is given by $1/\tau_{eff}$. Therefore, the rate of spontaneous emission is τ_{eff} /<n>. Using any of the approaches employed for evaluating γ_{ST} and $\Delta\omega_{CF}$ (e.g., references [34,35]), we find that the values of these quantities are given by Eq. (7) and (8), respectively, with τ_{eff} in place of τ_c. For I_0<<1, the value of τ_{eff} becomes larger by the factor of $1/I_0$, for the physical mechanism described above, thus implying that, near threshold, the STL becomes narrower for lower pump levels. We note that we are not aware of any experimental study that has been carried out to measure the value of γ_{ST} or the quantum noise limited value of $\Delta\omega_{CF}$ in this limit for a laser that has the idealized gain profile considered here.

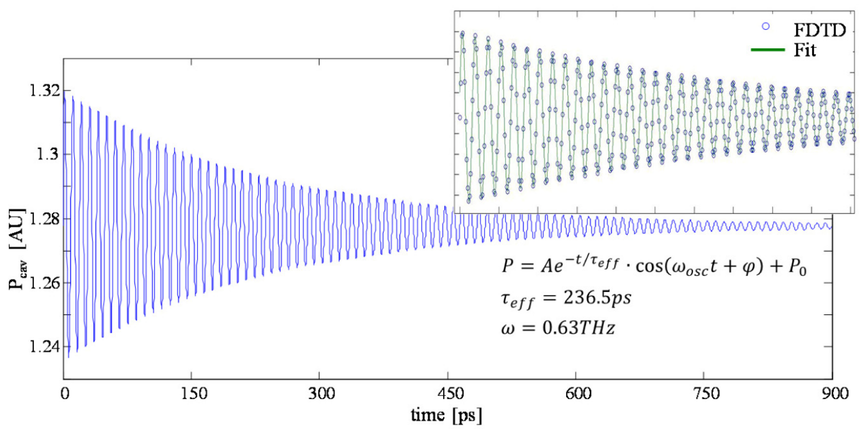

Fig. 11. Relaxation dynamics of a superluminal laser following a small perturbation. Inset: zoom in and fit to an oscillatory decaying function.

Figure 11 depicts the temporal dynamics of a superluminal laser with the parameters of Fig. 6 following a small perturbation. The power in the cavity oscillates where the amplitude of the oscillations is decaying over time. The inset of Fig. 11 depicts a fit of the power dynamics obtained by FDTD simulations to an oscillatory function with exponentially decaying amplitude. Excellent match is found for oscillation radial frequency of 0.63THz and exponential relaxation time constant of 236.5ps. This large decay constant is quite surprising. Even if the effect of the superluminal group velocity is disregarded and the impact of the non-saturated gain is taken into account, Eq. (11) predicts a substantially shorter relaxation time constant by approximately a factor of 4.5 ~52ps. Note that determining the relaxation time constant at higher pumping levels is not possible because the laser loses stability, as shown in Fig. 7. However, the study was repeated for a similar cavity except that the notch was less deep - $\Delta\varepsilon_A = -6.75\text{x}10^{-9}$, corresponding to $n_g \approx 0.45$. Because of the lower losses, the lasing intensity was higher and the resulting decay time was shorter ~78ps. Nevertheless, this time constant is substantially larger than the one expected from Eq. (11) (again, even if the effect of the superluminal group velocity is disregarded), which is ~15ps, again approximately a factor of 5 shorter. Thus, the larger than expected decay constant found from the FDTD simulations in the superluminal laser case is consistent. We also note that the oscillations are essentially a coherent effect which can be understood by the formation of two high-transmission peaks in the cavity around the resonance frequency due to the presence of the narrow absorption line located at the center of the gain line [22]. Specifically for the set of parameters of Fig. 11, calculation of the cavity transmission function according to Eqs. (5) and (6) yields two peaks at $\Delta\omega = \pm 0.31 THz$, corresponding to angular oscillation frequency of 0.62THz. This result agrees very well with the oscillation frequency obtained by the FDTD simulations (0.63THz).

Another important point to be taken from Fig. 11 is that the lasing solution of the superluminal laser (for this specific set of parameters) is dynamically stable. This is because the perturbation decays and the laser return to its original steady-state solution. Thus, we can conclude that there is a range of parameters in which stable superluminal lasing can be obtained. This result is very important as it indicates that such lasers can be used for highly-sensitive sensing applications [17,18].

A similar study was carried out for the superluminal laser with *saturating* absorption (see the dispersion relation in Fig. 8). Figure 12 depicts the temporal dynamics of that superluminal laser following a small perturbation. The general dynamics is similar to that depicted in Fig. 11 but with longer coherent relaxation time and slower oscillations. Due to the more complex nature of the saturating notch scheme (the system is highly nonlinear as both the gain and the absorption react to changes in the instantaneous lasing intensity) it is difficult to provide a simple explanation to the difference in the specific parameters. Nevertheless, the plot shown in Fig. 12 indicates that the superluminal lasing in this configuration is also stable against small perturbations.

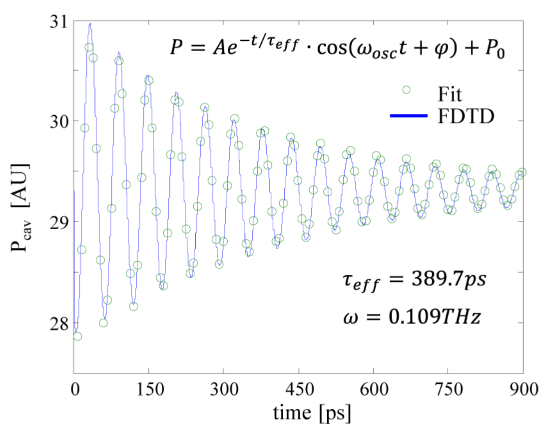

Fig. 12. Relaxation dynamics of a superluminal laser with *saturating* absorption following a small perturbation.

To complement the study of the superluminal laser dynamics we investigate the response of subluminal lasers to small perturbations. Figure 13 depicts the temporal dynamics of a subluminal laser with the following parameters: Γ_G = 6THz, Γ_A = 10GHz, $\Delta\varepsilon_G = 3.04\text{x}10^{-7}$, $\Delta\varepsilon_A = 2.5\text{x}10^{-10}$, $I_{sat}^G = 5$, and $I_{sat}^A = 500$. Following the perturbation, the power in the cavity relaxes exponentially to the steady-state level with a time constant of 146ps according to the fit. For comparison, the empty cavity lifetime is 16ps.

#251818 Received 12 Oct 2015; revised 8 Nov 2015; accepted 12 Nov 2015; published 8 Dec 2015

The long relaxation time can be understood from Eq. (11) when taking into account that the group velocity in the cavity is slower by n_g≈2.2 (see Fig. 4). The gain of the subluminal laser consists of two lines – a wide line with I_{sat} = 5 and a narrower line with I_{sat} = 500. The wide line is completely saturated (note that I_{ss} = 160) and, therefore, has negligible impact on the relaxation time while the narrow line is not. Thus, introducing into Eq. (11) I_0 = 160/500 and group index of 2.2 yields τ_{eff}≈145.5ps which is in very good agreement with the results of the FDTD simulations. To verify this good agreement we repeated the simulation with a wider additional gain line, Γ_A = 100GHz, which yields a lower group index - n_g≈1.1. The relaxation time obtained by the FDTD simulations was 57ps (I_{ss} = 210). Using Eq. (11) and including the group index we found that the expected relaxation time in this case is τ_{eff}≈59ps. Thus, it seems that the dynamics of the subluminal laser is described well by the conventional equations of motion with the impact of the group index and the gain saturation effects taken into account.

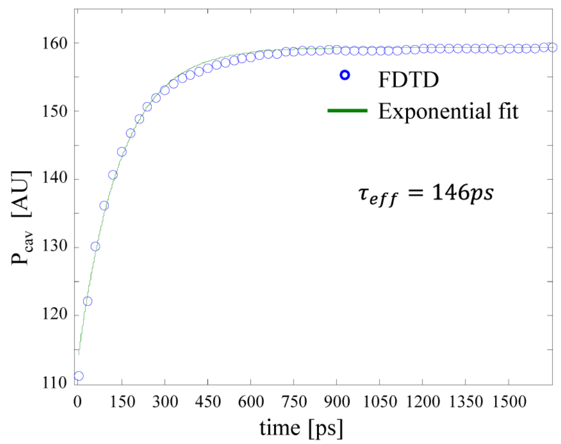

Fig. 13. Relaxation dynamics of a subluminal laser following a small perturbation and fit to an exponentially decaying function.

4. Conclusions

Super and sub-luminal lasers are interesting platforms which may find many applications in diverse fields, particularly sensing and metrology. We studied the dispersion properties and the dynamical response to power perturbation in such lasers using an FDTD simulation tool in an attempt to determine the range of parameters in which sub/super luminal lasing can be obtained. We found that while the properties observed for subluminal lasers agree well with the predictions of the self-consistent laser equations, the superluminal laser properties are more complex. We also found that obtaining superluminal lasing in the studied schemes (saturating and non-saturating absorption line) requires some care as it is necessary to introduce the dispersive element adiabatically in order to obtain stable solutions. Furthermore, we found that such solutions are more easily obtained close to lasing threshold and for group indices which are not entirely vanishing. Nevertheless, we did find a range of parameters for which such lasing is stable for group index as small as 0.14.

We studied the stability of superluminal and subluminal lasers to small perturbations, particularly the properties of the laser relaxation to steady state. By examining the case of a conventional laser we showed that this relaxation time constant is proportional to the empty cavity lifetime but it also depends on the ratio between the power in the cavity and the gain saturation power. While the dynamics of the subluminal laser seems to be relatively similar to those of conventional lasers, the dynamics found for the case of the superluminal laser schemes *studied here* is more complex. Specifically, in contrast to the subluminal laser case,

#251818 Received 12 Oct 2015; revised 8 Nov 2015; accepted 12 Nov 2015; published 8 Dec 2015

the relaxation time constant does not follow Eq. (11) and is surprisingly longer. In addition, the relaxation is accompanied by coherent oscillations which stem from the complex gain/loss spectral profile.

When considering the impact of intra-cavity dispersion on the cavity lifetime of these lasers, which is a necessary parameter for determining the STL, some caution in needed. While the dynamics of the subluminal laser is similar to that of a conventional laser, which may indicate that its STL is indeed reduced by the large group index, the dynamics found for the superluminal case is more complex. Particularly, the perturbation relaxation time constant of a superluminal laser is surprisingly larger than that of a conventional one (even when gain saturation effects are considered), which implies that the cavity lifetime in the superluminal case is longer. This inference is counterintuitive, as one might expect the lifetime of a superluminal cavity to be shorter than that of a conventional one. In addition, the impact of the oscillations on the spectral shape of the lasing line is not obvious as it may indicate a non-Lorentzian lineshape. Nevertheless, the fact that the relaxation time constant in superluminal lasers is not smaller than that of equivalent conventional lasers may indicate that the quantum-noise limited linewidth of such lasers is not broadened by the superluminal group velocity, thus rendering them attractive and feasible candidates for the realization of ultra-sensitive sensors and for measuring ultra-weak phenomena.

Acknowledgments

This research was partially supported by the Israel Science Foundation (Grant No. 364/10), and AFOSR Grant No. FA9550-10-1-0228, and NASA Grant No. NNM13AA60C.

#251818 Received 12 Oct 2015; revised 8 Nov 2015; accepted 12 Nov 2015; published 8 Dec 2015